

Shape Dependent Laplace Vortices in Deformed Liquid-Liquid Slug Flow

G.K.Kurup and Amar S. Basu *Member, IEEE*

Abstract— Understanding the hydrodynamics of liquid-liquid slug flow is important in the emerging field of plug-based microfluidics; however, the subtle aspects of the vortex geometry are still not comprehensively understood. This paper discusses the hydrodynamics of deformation dependent vortices that develop inside a water-in-oil slug as it flows through a channel. In contrast to prior studies, our simulations and experiments on slug flow reveal multiple vortices inside the moving slug, caused by the deformation of the hemispherical caps by Laplace pressures. These vortices appear in the front and rear of the plug at capillary number between 10^{-4} and 10^{-2} . A theoretical and simulation model shows the cause of asymmetry in slug deformation and the resulting vortices. Understanding the relevant parameters helps in optimizing slug flow for mixing and particle manipulation, which is important for plug-based microreactors and bead based assays.

I. INTRODUCTION

The plug based microfluidics also referred to as microreactors or microdroplets is potentially emerged as a system platform for performing high-throughput biomedical applications, explicitly in the field of biotechnology where samples are encapsulated in aqueous plugs or droplets in an immiscible carrier fluid. The plug is separated from the channel walls by a thin film of carrier fluid which forms if the surface tension between the plug and wall is greater than that of the carrier fluid and the wall [1]. In droplet based microreactors, recirculating flow occurs naturally inside the plugs caused by the relative displacement of plug and carrier fluid [2]. This recirculating flow pattern inside the plug is influenced by a several factors including flow velocity, plug length, channel size and viscosity ratio between the plug and carrier fluid [3, 4]. The recirculating flow can be utilized for effective mixing of reagents in different channel geometries [5, 6] and also for enhanced mass transfer [7]. The majority of prior experimental studies reported two recirculating vortices inside the plug [8]. In contrast to their findings, here we present simulation and experimental results which reveal multiple (4 or more) co-rotating vortices located at the front and rear of the plug. We refer to these as Laplace vortices because they are caused by the deformation of the

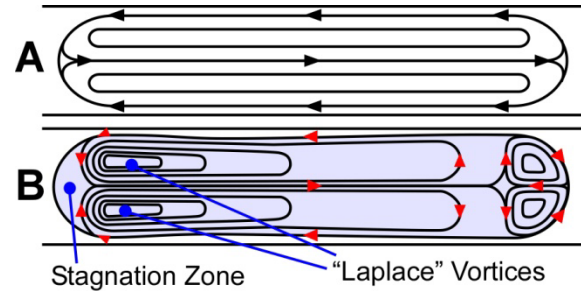


Figure 1: Comparison of (A) the classic model of slug flow and (B) deformation dependent slug flow

plug by Laplace pressures (Fig 1). Section II describes theory, section III the experimental setup, and section IV the results of CFD simulations and experiments.

II. THEORY

A. Basics of liquid-liquid slug flow

The two phase water-in-oil slug flow is encountered when water and oil flow simultaneously in a hydrophobic capillary over certain range of flow velocities. The pressure inside the plug is higher than the carrier phase due to the Laplace pressure differences; this pressure drives out the carrier fluid leaving a thin film around the plug. The thickness of the wetting film is given by Bretherton's classic paper [8] as

$$h = 1.34rCa^{2/3} \quad (1)$$

where h is the thickness of the film, and r is the capillary radius. The capillary number Ca is given by $\mu v/\gamma$, where μ is the viscosity of the carrier fluid, v is the velocity, and γ is the interfacial tension. It should be noted that Bretherton's law was originally derived for gas-liquid flow. Although recent papers in liquid-liquid flow cite this relation [3,7,9], it is acknowledged that this relation is only an estimate [3].

As a first step towards better understanding of complex plug flow, we developed an axisymmetric two phase flow model to demonstrate the impact of viscosity and film thickness on the velocity profile in the plug. This model considers the plug to be an infinitely long cylinder, and is therefore valid near the center of the plug. The slug flow in a circular pipe can be described as an axisymmetric Poiseuille flow with two concentric, coflowing phases with respective radii R_p and R_c and viscosities μ_p and μ_c respectively (Fig 2-A). The velocity at the axis and the droplet interface is given by solving the Poissuille/Hagen equation under a symmetric boundary condition at the axis, slip boundary condition at the interface, and a no-slip boundary condition at the wall. The solutions are:

Manuscript received March 23rd, 2010. This work was supported in part by the National Science Foundation.

G.K. Kurup is with the Electrical and Computer Engineering Department at Wayne State University, Detroit MI. A.S. Basu is with the Electrical and Computer Engineering Department and Biomedical Engineering Department at Wayne State University (e-mail: abasu@eng.wayne.edu, phone 313-577-3990).

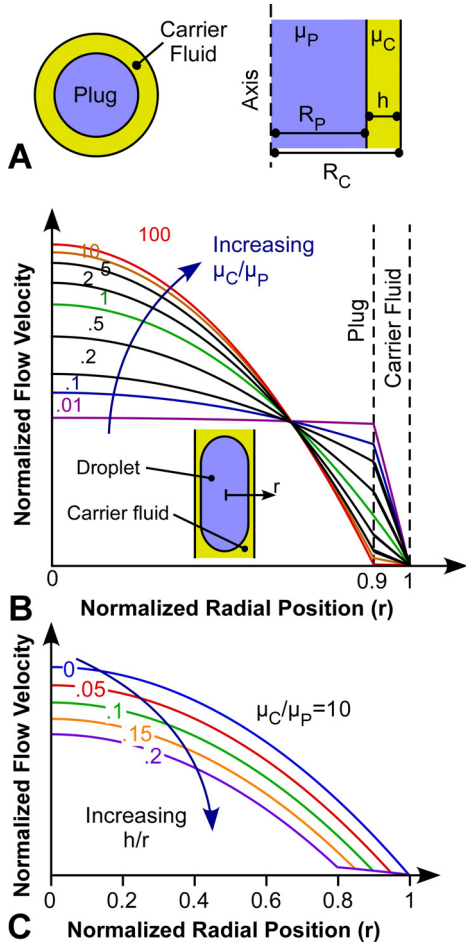


Figure 2: Axisymmetric poiseuille flow (A) Cross-sectional and longitudinal view of circular pipe. Radial distribution of velocity at the center of the plug at distinct range of (B) carrier phase viscosity and (C) film thickness

$$V(0) = \frac{1}{4} \frac{\Delta P}{\Delta x} \left(\frac{R_p^2}{\mu_p} - \frac{(R_p^2 - R_c^2)}{\mu_c} \right) \quad (2)$$

$$V(R_p) = -\frac{1}{4} \frac{\Delta P}{\Delta x} \left(\frac{R_p^2 - R_c^2}{\mu_c} \right) \quad (3)$$

$$V_{\text{circulation}} \sim V(0) - V(R_p) = \frac{1}{4} \frac{\Delta P}{\Delta x} \frac{R_p^2}{\mu_p} \quad (4)$$

Circulation in the plug ($V_{\text{circulation}}$) will occur if there is a velocity difference between the plug's axes, $V(0)$ and its edge, $V(R_p)$. Within the reference frame of the droplet, the circulation flow is reverse-oriented at the outer interface, and forward oriented in the interior region. The shape of the plug and shape dependent vortices depends on several factors including flow velocity, plug length, channel size, interfacial tension, and viscosity ratio between the plug and carrier fluid [4,10,11]. For example, it is found that a higher carrier phase viscosity results in increased velocity difference between the plug axis and its edge, leading to increased recirculation (Fig 2-B). This is because the shear exerted on plug boundary by the carrier phase increases with higher viscosity. Fig2-C illustrates the effect of the film thickness

on the velocity profile. A slight increase in the film thickness will reduce the shear force resulting in decreased velocity and the recirculation.

B. Origin of plug deformation and deformation dependent vortices

An interesting feature of the liquid-liquid slug flow is that at higher capillary number the slug deforms due to the Laplace pressure difference which exists along the length of the plug. The Laplace pressure is $\Delta P = \gamma(R_1^{-1} + R_2^{-1})$ where γ is the interfacial tension and R_1 and R_2 are the radii of curvature. At the front and the rear end of the plug, due to the two-axis curvature of the hemispherical cap, the Laplace pressure is given by the equation $\Delta P = 2\gamma(R_1^{-1})$. At the center of the plug, where there is a single axis curvature (R_2 approaches infinity), the Laplace pressure is given by $\Delta P = \gamma(R_1^{-1})$. The spatial variations in Laplace within the plug play a major role in determining the flow patterns inside the plug [12], although the specific mechanisms are still under investigation.

Deformation dependent vortices are asymmetric vortices that appear at either ends of the plug due to the deformation of its shape. We refer to these as ‘‘Laplace’’ vortices because their origin is due to the Laplace pressure. The bulging of the plug near the caps reduces the thickness of the lubricating film, generating increased surface shear and recirculating flow in these regions.

III. EXPERIMENTAL SETUP

A. CFD Model

We have established a CFD model (COMSOL 4.0) for the qualitative and quantitative analysis of the hydrodynamic flows in the plug. COMSOL 4.0 utilizes a modified level-set method to track the liquid-liquid interface. This model provides a more accurate calculation of surface tension force than the traditional volume-of-fluid (VOF) method [13], which is critical for calculating droplet deformation and resulting Laplace vortices. It also provides accurate mass conservation compared to the traditional level set method. The multiphase model accounts for interfacial tension between the plug and carrier fluid, relative viscosities, Laplace pressure, and the hydrophobicity of the channel walls, all of which play a significant role in liquid-liquid slug flow[14]. The multiphase model helps understand the geometry of flow and how it changes in response to materials and geometric parameters.

B. Experimental

To experimentally characterize the water-in-oil slug flow, plugs of required length on demand are generated using syringe pump, commercial tee junction and transparent PTFE capillary tubing of internal diameters 200 μm and 500 μm . To investigate the effect of carrier fluid (viscosity and surface tension) on the deformation dependent vortices, studies has been conducted on silicone oil (1 and 10 cst, $\gamma = 30$ mN/m), oleic acid (~ 20 cst, 30 mN/M), and fluorinated fluid (FC3283 ~ 1 cst, FC70 ~ 12 cst, $\gamma = 54$ mN/M). In order to visualize the flow pattern and to track the existence of

vortices, monodisperse fluorescent particles of diameters ranging from 0.1-10 μm (Polysciences) are suspended in the aqueous phase. The plug length, velocity profile and the concentration profile within the slug are observed using stroboscopic fluorescent particle image velocimetry. The system consists of 150 mW, 405 nm pulse-modulated laser, dichroic mirror, 20X objective, microchip/specimen and CCD camera which detects the fluorescent signal emitted from the sample (Fig 3). The ratio of the pulsed laser frequency to the shutter speed of the camera determines the number of points imaged in each frame which can be used directly to calculate the velocity of the particles. For example, a laser frequency of 300 Hz and a camera exposure time of 10ms will result in 3 particle snapshots per frame.

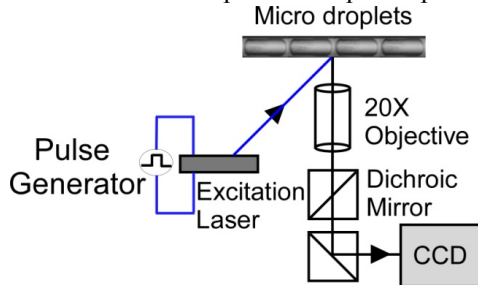


Figure 3: Stroboscopic particle image velocimetry system

IV. RESULTS AND DISCUSSION

This section gives experimental evidence of Bretherton films, deformation of plugs, and the existence of deformation dependent vortices.

A. Bretherton Films in liquid-liquid slugs

Although Bretherton's law of film thickness is ideally suited for gas-liquid slug flow, our analysis shows it is reasonably valid in the case of liquid-liquid slug flow. The h/r ratio of the front end and rear end of the plug (shown in Fig. 5B) is measured and plotted against the capillary number (Fig. 4). These curves are compared with the ideal Bretherton's equation (red dotted curve). Our result revealed close correlation with the studies of Hodges [14] which stated that the film thickness is proportional to $Ca^{2/3}$, regardless of whether the drop is viscous or inviscid. Deformation of the plug can result in spatial variation in the film thickness between the front and rear end of the plug.

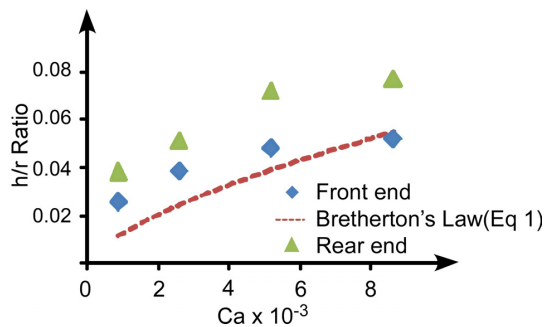


Figure 4: Measured thickness of Bretherton films in a deformed slug. The front and rear end film thickness is experimentally determined and plotted against the capillary number. Theoretical values are shown in red.

B. Plug deformation

Plug deformation (Fig. 5) is observed both in CFD and experiments. A CFD model of the plug (figure 5A) is simulated at a velocity of 100 mm/s with kinematic viscosity and interfacial tension of 10 cst and 30 mN/m respectively. The model shows a deformation where the rear of the plug is thinner than the front. The deformation is caused by the Laplace pressure variations which occur within the plug. In experiments (Fig. 5B), the deformation is much smaller and is only observable under a narrow range of experimental parameters. These parameters include plug length, plug velocity, viscosity ratio, and interfacial tension. In the case of very low capillary number and short plugs, the deformation is almost negligible. The experiment is carried out at plug velocity of 12 mm/s with kinematic viscosity and interfacial tension of 12 cst and 54 mN/m respectively. The deformation is axially symmetric because the Laplace pressure differences also exist symmetric throughout the plug. The existence and geometry of the vortices coincides with the deformation of the plug; hence, we refer to them as 'deformation-dependent vortices'.

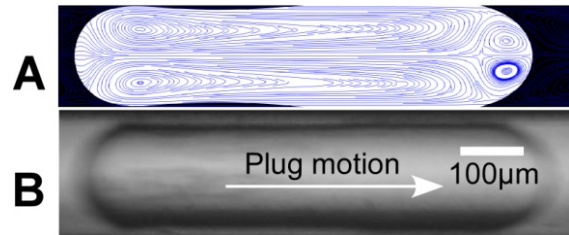


Figure 5: Comparison of (A) CFD modeling of slug deformation, (B) Deformation observed in experiments.

C. Deformation-Dependent Vortices

Deformation Dependent Vortices (*DDV*) are those vortices which appear due to the deformation of the plug. Figure 6 illustrates the rear end Laplace vortices in both simulations and experiments. The simulation results is shown in Figure 6A, which is carried out at a velocity of 50 mm/s with kinematic viscosity and surface tension of 10cst and 30 mN/M respectively. It is important to note that these vortices are located adjacent to the caps of the plug, where bulging of the plug occurs. In this region, the Bretherton film is thinner than the surrounding areas. As shown earlier in Figure 2C, even a small decrease in the thickness of the lubricating film will cause a local increase in the tangential shear force. The spatial variation in this shear force results in vortex flow near the caps.

In the experiments, in order to visualize the vortices, 10 μm fluorescent beads are suspended in the plug and the particle movement in the vortices is captured using our custom stroboscopic imaging system. The agglomeration of the particle in the rear Laplace vortex as the slug moves through the capillary is shown in Figure 6B. The agglomeration corresponds with the location of the vortices.

D. Dependence of Laplace vortices on capillary number

The effect of capillary number (at fixed plug length) on the geometry of the Laplace vortices was investigated through CFD simulations and experiments. The simulation

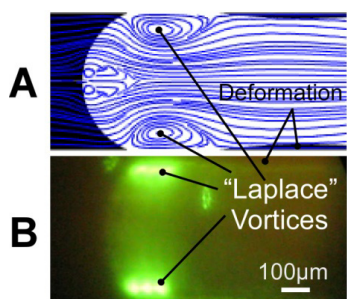


Figure 6: (A) Rear Laplace vortices in CFD simulation (B) 10 μm fluorescent beads trapped in rear end Laplace vortices at plug velocity of 6mm/s through a 500 μm capillary.

model (Fig. 7) shows that in medium sized plugs ($l/w < 5$), the geometry of the front Laplace vortices depends on the capillary number, which is proportional to velocity. As Ca is increased, the vortex becomes smaller in length and more localized toward the front of the plug. This is believed to be due to increases in shear forces and slight deformations in the plug shape.

In experiments (Fig. 8), clear and distinct vortices develop in the plug (500 μm ID tubing) for capillary number in the range of $10^{-4} < Ca < 10^{-2}$, the same range as simulations. However, at very low capillary number in the range of 10^{-5} , the recirculation is completely absent. Gradually increasing the capillary number to 10^{-3} results in the progressive improvement in the recirculation. Above $Ca \sim 10^{-1}$, the vortices are replaced with bypass flow (no circulation).

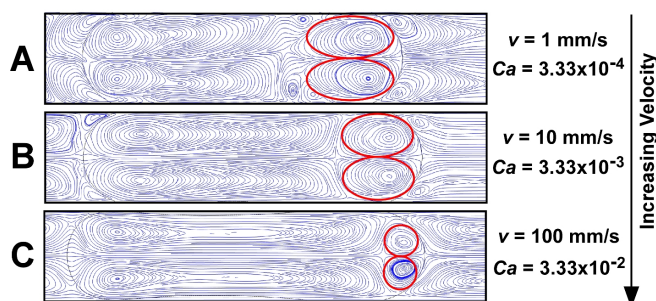


Figure 7: CFD simulations illustrating the dependence of Laplace vortex geometry (circled in red) on flow velocity.

V. CONCLUSION

This paper has shown that in slug flow microfluidics, the plug deforms due to the difference in the Laplace pressure along the length. This deformation results in varied film thickness which alters shear force at the boundary and hence generate multiple vortices also referred as Laplace vortices. The flow profile and the vortex geometry in the plug is a complex phenomenon which depends on various operational parameters specifically, the capillary number, plug length and channel geometry. Understanding this phenomenon helps in manipulating the vortex flows and could potentially be used for mixing and concentrating particles, which can lead to numerous applications in high throughput screening.

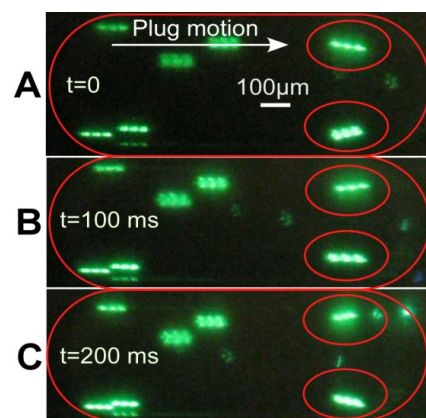


Figure 8: Visualization of 10 μm particle motion in front Laplace vortices by stroboscopic particle image velocimetry with laser pulse rate 300 Hz.

REFERENCES

1. J. Bico and D. Quéré, "Self-propelling slugs," *Journal of Fluid Mechanics*, vol. 467, 2002
2. S.R. Hodges, O.E. Jensen and J.M. Rallison, "The motion of a viscous drop through a cylindrical tube", *Journal of Fluid Mechanics*, vol. 501, pp. 279-301
3. A. Ghaini, A. Mescher, and D.W. Agar, "Hydrodynamic studies of liquid-liquid slug flows in circular microchannels," *Chemical Engineering Science*, vol. 66, 2011, pp. 1168-1178..
4. M.N. Kashid, I. Gerlach, S. Goetz, J. Franzke, J.F. Acker, F. Platte, D.W. Agar, and S. Turek, "Internal Circulation within the Liquid Slugs of a Liquid-Liquid Slug-Flow Capillary Microreactor," *Industrial & Engineering Chemistry Research*, vol. 44, Jul. 2005, pp. 5003-5010
5. H. Song, D.L. Chen, and R.F. Ismagilov, "Reactions in droplets in microfluidic channels," *Angewandte Chemie International Ed*, vol. 45, 2006, p. 7336.
6. J.D. Tice, H. Song, A.D. Lyon, and R.F. Ismagilov, "Formation of Droplets and Mixing in Multiphase Microfluidics at Low Values of the Reynolds and the Capillary Numbers," *Langmuir*, vol. 19, 2003, pp. 9127-9133
7. M. Kashid and D. Agar, "Hydrodynamics of liquid-liquid slug flow capillary microreactor: Flow regimes, slug size and pressure drop," *Chemical Engineering Journal*, vol. 131, 2007, pp. 1-13.
8. F.P. Bretherton, "The motion of long bubbles in tubes," *Journal of Fluid Mechanics*, vol. 10, 1961, p. 166
9. M.N. Kashid, D.F. Rivas, D.W. Agar, and S. Turek, "On the hydrodynamics of liquid-liquid slug flow capillary microreactors," *Asia-Pacific Journal of Chemical Engineering*, vol. 3, 2008, pp. 151-160.
10. C. King, E. Walsh, and R. Grimes, "PIV measurements of flow within plugs in a microchannel," *Microfluidics and Nanofluidics*, vol. 3, 2007, pp. 463-472.
11. T.C. Thulasidas, M.A. Abraham, and R.L. Cerro, "Flow patterns in liquid slugs during bubble-train flow inside capillaries," *Chemical Engineering Science*, vol. 52, Sep. 1997, pp. 2947-2962.
12. C. N. Baroud, F. Gallaire, and R. Danga, "Dynamics of microfluidic droplets," *Lab on a Chip*, vol. 10, no. 16, p. 2032, 2010.
13. M. Kashid, A. Renken, and L. Kiwi-Minsker, "CFD modelling of liquid-liquid multiphase microstructured reactor: Slug flow generation," *Chemical Engineering Research and Design*, vol. 88, 2010, pp. 362-368.
14. A. Ufer, M. Mendorf, A. Ghaini, and D.W. Agar, "Liquid/Liquid Slug Flow Capillary Microreactor," *Chemical Engineering & Technology*, 2011, pp. 353-360.